Arabian Journal of Chemistry (2020) 13, 1731–1740

King Saud University

Arabian Journal of Chemistry

www.ksu.edu.sa
www.sciencedirect.com

ORIGINAL ARTICLE

Novel chitosan/polyvinyl alcohol thin membrane adsorbents modified with detonation nanodiamonds: Preparation, characterization, and adsorption performance

Vahid Vatanpour [a], **Ehsan Salehi** [b,*], **Nadia Sahebjamee** [c], **Mahbubeh Ashrafi** [d]

[a] *Department of Applied Chemistry, Faculty of Chemistry, Kharazmi University, 15719-14911 Tehran, Iran*
[b] *Department of Chemical Engineering, Faculty of Engineering, Arak University, Arak 38156-8-8349, Iran*
[c] *Department of Chemical Engineering, Quchan Branch, Islamic Azad University, Quchan, Iran*
[d] *Petrochemical Research and Technology Company, Pajoohesh Avenue, P.O. Box 1435884711, Tehran, Iran*

Received 22 October 2017; accepted 21 January 2018
Available online 1 February 2018

KEYWORDS

Adsorption;
Membrane adsorbent;
Nanodiamonds;
Heavy metals;
Isotherm

Abstract Detonation nanodiamonds (DNDs), for the first time, were utilized to modify chitosan/polyvinyl alcohol (CS/PVA) thin membrane adsorbents. For this purpose, different contents of DNDs, from nil to 1.5 wt%, were embedded in the polymer matrix of the membranes to obtain the optimum content. Static adsorption of Pb(II) on the prepared membrane adsorbents was studied. The fabricated membranes were characterized in terms of morphology and performance using scanning electron microscopy (SEM) micrographs and Fourier transform infrared (FTIR) spectrum analyses. Langmuir and Freundlich isotherms were used to model the equilibrium adsorption. The effects of pH, temperature, and initial metal concentration on the adsorption capacity were investigated. Results showed that adsorption of lead ion is more favorable at pH = 6. Thermodynamic parameters including ΔH^{o}, ΔS^{o} and ΔG^{o} revealed endothermic, entropy-driven and spontaneous nature of the adsorption. Adsorption capacity for Pb(II) increased from 29.5 mg g^{-1} (for the plain membrane) to 121.3 mg g^{-1} by the addition of 1.5 wt% DNDs; however, the optimal content was 1 wt% DNDs considering both mechanical stability and adsorption capacity. Results revealed that the ultra-thin CS/PVA membrane adsorbents modified with DNDs are very potential candidates for heavy metal adsorption.

* Corresponding author.
E-mail addresses: ehsan1salehi@gmail.com, e-salehi@araku.ac.ir (E. Salehi).

Peer review under responsibility of King Saud University.

Production and hosting by Elsevier

https://doi.org/10.1016/j.arabjc.2018.01.010
1878-5352 © 2018 Production and hosting by Elsevier B.V. on behalf of King Saud University.
This is an open access article under the CC BY-NC-ND license (http://creativecommons.org/licenses/by-nc-nd/4.0/).

1. Introduction

The appearance of heavy metals in wastewater is conducive to long-term risks in the ecosystem. One of the most dangerous heavy metal ions, which enter the environment via industrial effluents, is lead. The sources of releasing lead into the environment are battery manufacturing, acid metal plating and finishing, ammunition, tetraethyl lead manufacturing, ceramic and glass industries, printing, painting, dying, and other related industries (Ridha, 2017). Lead is non-biodegradable and tends to bio-accumulate in the cells of the living organisms. Exposure to lead may lead to anemia, severe problems with the nervous system, failure of reproductive system, liver and kidney diseases, brain damage and ultimately death (Gupta et al., 2011). Therefore, removing lead ions from water resources is very important, even at low concentrations (more than 0.01 mg/L) (Mehdipour et al., 2015).

Membrane separation technology compared to the conventional separation processes has much superiorities including lower power consumption, smaller footprint, ability of being manufactured with different sizes and modules, favorable mass transport, lower pressure drop, usability for materials sensitive to temperature, regeneration capacity, high efficiency, easy scale-up and ability to be hybridized with other separation processes (Mehdipour et al., 2015).

Recently, membrane adsorption has appeared as a popular technology to remove heavy metal ions from effluents (Gupta et al., 2011). The membrane adsorption compared with conventional separation methods such as chemical precipitation, ion exchange, and adsorption columns offers unique advantages for the heavy metals removal. Some examples of relative advantages of membrane adsorption are high removal efficiency especially at low metal concentration, normal productivity, low-pressure drop, proper reusability, fast kinetics and desired removal rate (Mehdipour et al., 2015; Salehi and Madaeni, 2014). The existence of abundant functional groups such as $-COOH$, $-OH$, $-NH_2$ and $-SO_3H$ on the surfaces of the adsorptive membranes makes them chemically so reactive. The functional groups are capable to adsorb heavy metal ions through surface complexation, chemical bonding and/or ion-exchange mechanisms (Salehi and Madaeni, 2014). In addition, membrane adsorbents are ultra-thin film adsorbers, usually with the average thickness less than 20 μm (Salehi and Madaeni, 2014). Having these characteristics provides the conditions for facilitated and enhanced mass transport through the membranes. Accordingly, heavy metal ions can be favorably adsorbed by the membranes even at trace concentrations (less than 10 mg/L).

Chitosan (CS) is a well-known natural polysaccharide, the second most available biopolymer in nature, with a wide range of applications in the preparation of adsorptive membranes. This polymer has excellent properties such as high hydrophilicity, normal chemical resistance, abundant reactive functional sites, biocompatibility and biodegradability (Salehi et al., 2016). Chitosan contains amine and hydroxyl functional groups; meanwhile, the amine groups are in advance responsible for chelating heavy metal ions (Jayakumar et al., 2011).

The combination of chitosan with suitable polymers such as cellulose acetate, acrylonitrile butadiene styrene, and polyvinyl alcohol have also resulted in highly reactive and mechanically stable membranes (Jayakumar et al., 2011; Shawky, 2009). Polyvinyl alcohol (PVA), a highly hydrophilic and CS-compatible polymer, has been extensively used to enhance the mechanical and chemical properties of chitosan membranes (Cheng et al., 2010; Liu and Bai, 2006; Jin and Bai, 2002).

Except for porosity and morphology, the addition of nanostructures can promote the sorption properties of chitosan membrane adsorbents. Incorporation of inorganic nanoparticles can also improve the mechanical properties of the membranes (Ashori and Bahrami, 2014; Delavar and Shojaei, 2017; Ghaee et al., 2010; Khabashesku et al., 2005; Khan et al., 2017; Vatanpour et al., 2012; Zarghami et al., 2015). Acid functionalized CNTs embedded into CS/PVA adsorptive membranes were studied by Zarghami et al. for adsorption of Pb(II) and Zn(II) ions (Zarghami et al., 2015). Peng et al. Modified nanoporous magnetic cellulose–chitosan microspheres by adding abundant carboxyl groups for efficient removal of Pb(II) from aqueous solution (Peng et al., 2017). Chitosan grafted with poly(itaconic acid) were synthesized by Kyzas et al. to enhance the lead ion uptake by the chitosan adsorbent (Kyzas et al., 2014). Chitosan schiff's base@Fe_3O_4 were fabricated and used for the removal of Pb(II) ions from aqueous solutions in batch adsorption mode. Chitosan was modified by crosslinking with aldehyde and ZnO in this work (Weijiang et al., 2017). Chen et al. synthesized xanthate-modified magnetic chitosan/PVA particles as a novel adsorbent (Lv et al., 2017). This modification could elevate the mechanical stability, reusability and adsorption properties of the chitosan adsorbent.

Nanodiamonds have emerged as promising nanoparticles because of their remarkable mechanical, thermal and biological properties together with its large specific surface area (larger than 200 m^2/g) and hydrophilic surface owing to the presence of many oxygenated functional groups (Delavar and Shojaei, 2017). Khabashesku et al. (2005) showed that nanotubes and nanocrystalline diamond powders need some surface modifications due to lack of interfacial bonding and nonreactive surface.

On July of 1963, the Soviet Union and East Block discovered detonation synthesis method for producing nanodiamonds (Danilenko, 2004). The detonation nanodiamonds (DNDs) produced by detonation synthesis are called explosive nanodiamonds or ultra-dispersed nanodiamonds, which are uniform spherical nanoparticles with an average size of 4–6 nm and have a large and accessible surface area. The X-ray diffraction (XRD) analysis have shown that the DNDs nanoparticles have the cubic structure with lattice constant a = 0.355 nm and density of 3.05–3.4 g/cm^3 (Dolmatov, 2001; Gerasin et al., 2013). The nanoparticles also preserve and show most of the unique properties of diamond such as excellent hardness, high specific surface area, thermal conductivity, optical properties, biocompatibility, stability and good chemical resistance even at environments with harsh conditions (Dolmatov, 2001; Mochalin et al., 2012). The DNDs are considered from the category of tough synthetic powders, which are derived from the reaction of two materials that are more explosive, the nitro toluene and the hexogen with certain ratios. The presence of a large number of different functional groups on the surface of the DNDs is another distinguished property of these nanoparticles compared to other nanoparticles (Delavar and Shojaei, 2017; Behler et al., 2009; Zhang et al., 2010).

In this study, the DNDs are used, for the first time, to modify chitosan/PVA adsorptive membranes in order to improve the adsorptive removal of lead ions from aqueous solutions. SEM and FTIR analysis were employed to characterize the membranes containing different nanostructure contents. Batch adsorption experiments were conducted to study the adsorption isotherms and thermal effects.

2. Materials and methods

2.1. Chemicals

Chitosan powder with 90% deacetylation degree and molecular weight of 100,000–300,000 Da was purchased from Acros. Polyvinyl alcohol (PVA, Mw = 58,000 Da) from Merck (Germany) was used for membrane fabrication. Spherical nanodiamond particles were prepared from PlasmaChem Company (Germany). All other chemicals were of analytical grade and used without further purification.

2.2. Apparatus

An ultrasound sonicator (SONOREX DIGITE DT255BANDELIN) was employed for homogeneous dispersing of DNDs in aqueous solutions. A thermal shaker-incubator (NB-205V) was used to keep temperature fixed during batch adsorption experiments. A heater stirrer (IKA WERKE) was used to keep the solution at a constant temperature and constant stirring solution.

The Fourier transform infrared (FTIR) spectrum was performed by a Fourier transform infrared spectrometer (Brucker VERTEX 80, Germany). To determine the concentration of lead ions in the sample solution, an inductively coupled plasma (ICP) spectrometer (Varian MPX Vista model) was applied.

Morphology of the membranes was characterized using a scanning electron microscopy (SEM, VEGA, Tescan). The image of the fabricated membranes was observed at accelerating voltage of 10 kV. For removal of probably attached contaminants, the membranes were cut to the small coupons and cleaned by filter paper. For cross-sectional scanning, the coupons were immersed in liquid nitrogen to freeze. Following, the frozen parts were broken and coated with a gold conductive layer.

2.3. Membrane fabrication

To prepare chitosan/polyvinyl alcohol membrane adsorbents, CS and PVA solutions were prepared separately and then, mixed. Firstly, 1% (v/v) acetic acid solution was prepared. Afterwards, distinct amount of chitosan powder was added to the above solution with stirring (150 rpm) at room temperature for 24 h to obtain a 2 wt% CS solution.

The nanodiamonds with different percentages of 0.2, 0.5, 0.75, 1.0, 1.25 and 1.5 wt% relative to the total weight of all the polymers used (PVA and chitosan) were added to 10 wt % PVA sample solution. For this purpose, different amounts of the DNDs were added to 9 g of water and ultrasonicated for 30 min for appropriate dispersion. Next, PVA granules (1 g) were added to the above solutions. The PVA/DNDs solutions were heated at 70 °C using an oil bath for 24 h under constant stirring (150 rpm) to obtain homogenous solution. After 24 h, the chitosan and PVA solutions were mixed and heated at 50 °C in the oil bath for 1 h under constant stirring (250 rpm). The obtained solutions were kept in the bath without stirring for 48 h at 50 °C to sufficiently free from the air bubbles and crosslinked. After that, the prepared solutions were cast on glass plates using a film applicator with the thickness of 250 μm and allowed to dry at room temperature overnight. The dried films attached on the glass plates were immersed into 1 M NaOH solution for 1 h to separate the membranes from the glass surface. Finally, the obtained membranes were carefully rinsed with distilled water and then left to dry for 24 h at room temperature.

2.4. Static adsorption

To measure the equilibrium adsorption of the prepared membrane, 50 mL lead solutions with different concentrations (1, 2, 5, 10, 20 and 30 mg/L) were incubated with distinct mass of the membrane adsorbent (~0.02 g) under constant stirring (150 rpm) for 24 h. pH for adsorption of Pb(II) ions on the CS/PVA membranes was adjusted between 4 and 6 (4, 5 and 6). Firstly, adsorption tests of all the samples were conducted at pH = 6 and 20 °C. Then, two other temperatures (30 and 40 °C) as well as different pH values (4 and 5) were tested using the membranes with the optimum percentage of the nanodiamonds. The concentration of the ions in the feed and supernatant solutions was measured using ICP spectrometer. Equilibrium adsorption was determined according to the following equation:

$$Q_e = \frac{(C_0 - C_e)}{m} V \quad (1)$$

where Q_e is the equilibrium adsorbed amount of Pb(II) ions on the membrane (mg/g), V is the volume of the solution (L), C_0 and C_e are the initial and final concentrations of Pb(II) ions (mg/L) in the solutions, respectively, and m is the mass of the adsorptive membrane (g).

3. Results and discussion

3.1. Characterization of nanodiamonds (DNDs)

3.1.1. FTIR analysis of DNDs

FTIR spectral analysis was performed to confirm the functional groups on the nanoparticle surface. A Brucker VERTEX 80 FTIR spectrometer was employed for this purpose. Oxygen-containing functional groups such as hydroxyl, carboxyl and ether are created on the surface of nanodiamonds when the nanoparticles are produced through detonation synthesis (Krueger, 2008). In Fig. 1, FTIR spectrum is related to DNDs. A strong peak appears as one broad band in the region of 3300–3500 cm^{-1}, which is attributed to the stretching vibration of O—H groups. The 2830–2930 cm^{-1} peak is related to the symmetric and asymmetric stretching vibration of C—H groups (Mitev et al., 2007). The stretching vibration of C=O belongs to carbonyl and carboxyl groups and appears at 1708 cm^{-1}. The bending vibration of O—H groups, also stretching vibration of aromatic carbon graphite SP^2 linked around the nanoparticle appear at 1628 cm^{-1}, whereas, the

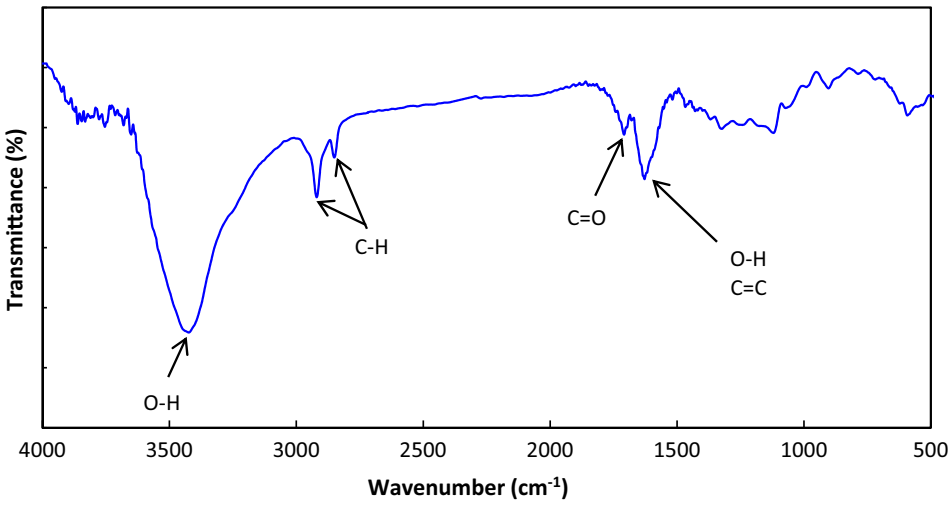

Fig. 1 FTIR spectra of DNDs nanoparticles.

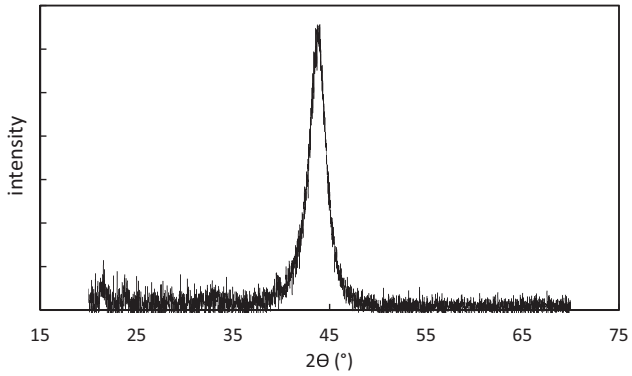

Fig. 2 XRD spectra of the DNDs nanoparticles.

stretching vibration of the ether C—O appeared at 1120 cm^{-1} (Mochalin et al., 2012; Mitev et al., 2007).

The IR spectrum of most nanoparticles which have been synthesized by detonation technique, a broad absorption band in the region 1000–1500 cm^{-1} is visible, which is known as the fingerprint area (Zarghami et al., 2015). This fingerprint area is related to the stretching vibration of C—C, C—O—C, the stretching vibration of an amide C—N, vibrations of C—N—H and the vibrations of NO_2. In this method, the nanoparticles are produced from the reaction between two highly explosive material e.g. nitro toluene and hexogen, therefore it is quite possible that nitrogen compounds residual remains in the structure of the nanodiamonds (Mochalin et al., 2012).

3.1.2. XRD spectra of the DNDs nanoparticles

In order to observe the accuracy of DNDs construction, X-ray diffraction method is used. Fig. 2 shows an XRD pattern of the nanodiamonds. The XRD analysis was performed using a powder diffractometer. The pattern shows a peak at an angle $2\theta = 43.66°$ which is related to the face-Centered Cubic (FCC) structure of the diamond with space group of 227 and constant lattice A° of a = 3.566 (Morimune et al., 2011). The phase identification, which has been done by XRD analysis, confirms this crystal structure. The diamond structure includes two networks with face-Centered Cubic, which have influence on each

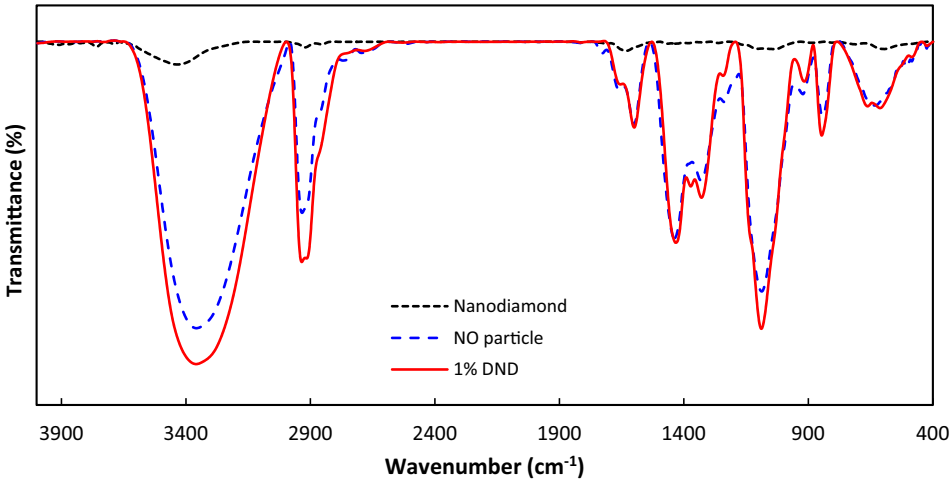

Fig. 3 ATR-FTIR transmission spectra of DNDs, plain membrane and membrane with 1% nanodiamond.

other. In this structure, there are eight carbon atoms and each carbon atom bonding to four others covalently (Morimune et al., 2011; Evarestov, 2012; Lee and Lim, 2004). This suggests that diamond nanoparticles, even with less than 10 nm size, have three-dimensional structure.

3.2. Membrane characterization

3.2.1. FTIR analysis

FTIR analysis was performed for the raw nanodiamonds, the membrane samples without nanoparticles and with 1% nanodiamonds. The results are depicted in Fig. 3. The wavelength of 3360 cm^{-1} is related to stretching vibrations of polyvinyl alcohol —OH group, and chitosan —NH_2. Stretching vibration of C—H appeared at 2935 cm^{-1}, whereas, 1089 cm^{-1} is related to C—N bond of chitosan and C—O bonds of polyvinyl alcohol and nanodiamonds (Salehi et al., 2012).

Comparing the plain membrane with the membrane containing 1% nanodiamonds shows an increase in absorbance at wavelength of 1089, 2935 and 3360 cm^{-1}. These peaks also appear in the nanodiamonds spectra. This confirms the existence of the nanoparticles in the CS/PVA membrane structure. Increased intensity of the peaks represents an increase in the membrane functional groups. These functionalities can act as reactive adsorption sites and enhance the adsorption of Pb (II) from the aqueous media.

3.2.2. SEM micrographs

SEM is a widely used technique to study the cross-section morphology and surface characteristics of membrane adsorbents (Nesic et al., 2012). Fig. 4 shows SEM images of the membrane samples with different contents of DNDs (0, 0.5, 1.0, 1.5 wt%). The average thickness of the prepared membranes is around 5 μm which is smaller than the average thickness of the film adsorbents (10 to 20 μm) based on literature (Salehi and Madaeni, 2014; Salehi et al., 2012; Salehi et al., 2013). Accordingly, the fabricated membranes are classified as ultra-thin film adsorbents. The images of the membrane surfaces Fig. 4a–h) clearly show that a homogeneous dispersion of DNDs is achieved throughout the CS/PVA matrix (He et al., 2014). Some protuberances can be observed in Fig. 4b and c, indicating that DNDs rather tend to aggregate during preparation of composite films (Zuo et al., 2013). Fig. 4d depicts that, with the addition of nanoparticle percentage, the nanoparticle content increases on the membranes surface. Undesirable agglomeration of the nanodiamonds on the membrane surface can be caused by side interactions between functional groups on the nanoparticles surface. Fig. 4c shows the optimal membrane with uniform distribution of DNDs.

Fig. 4d shows that embedding 1.5% DNDs leads to agglomeration of DNDs on the membrane surface, which it makes the membrane quite fragile. In addition, application of CS/PVA membranes with 1.5% DNDs for adsorption is limited due to weak structure and unfavorable mechanical properties. The resulted membranes with 1.5% DNDs were also very hard to produce and we able to difficultly cut the membranes to certain area. The density of the blended membranes increased apparently compared to the plain membrane. This indicates the strong interaction among the CS and PVA polymers and DNDs.

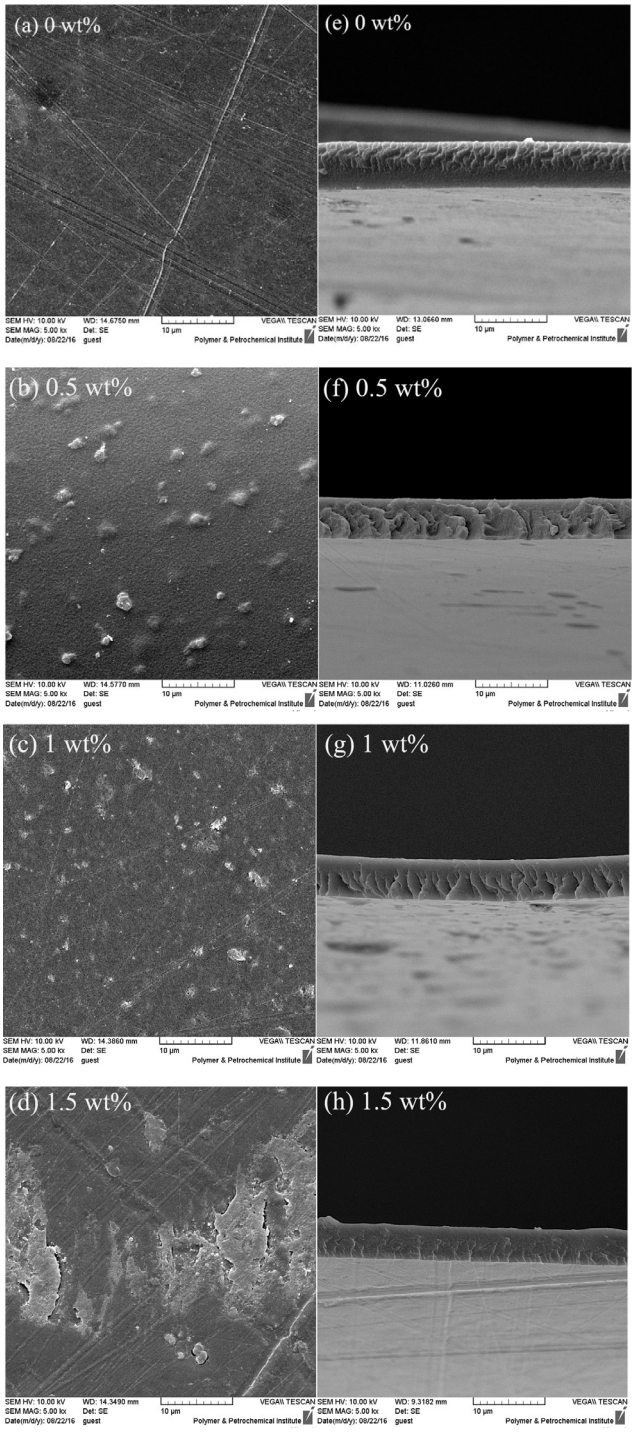

Fig. 4 Surface (a–d) and cross-section (e–h) SEM images of CS/PVA membranes with different DNDs contents.

The cross-sectional SEM images of the membranes containing various amounts of DNDs are depicted in Fig. 4d–h. The cross-sectional images of the membranes demonstrate clear stratification as bright lines in their structures (Salehi et al., 2012; Salehi et al., 2013; Han et al., 2011). With the addition of nanodiamonds in the membrane matrix, the membrane pore density and porosity increases which may cause a rise in the adsorption content due to the increase of the effective surface

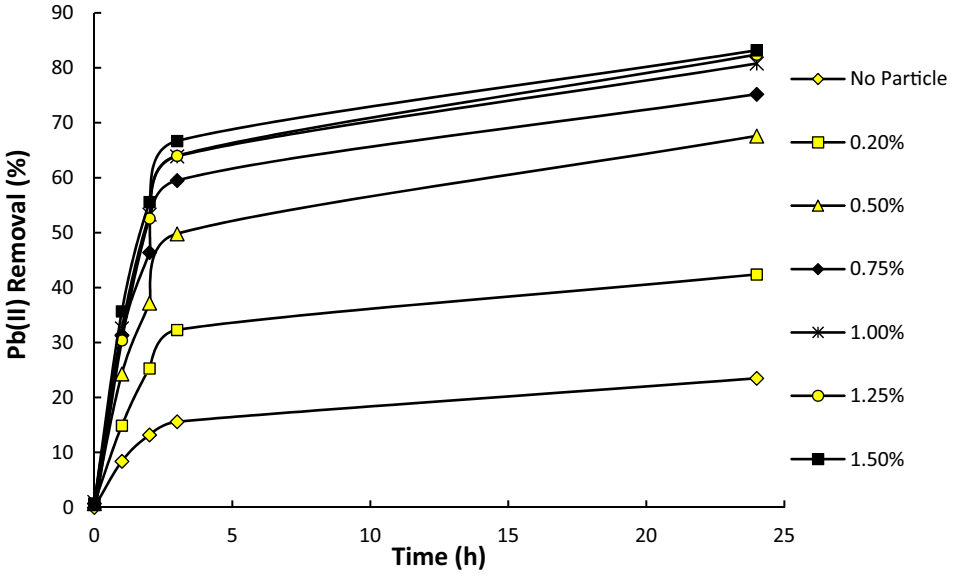

Fig. 5 Effect of different percentages of DNDs on the removal of Pb(II) during 24 h (Pb(II) concentration = 30 ppm, 30 °C and pH = 6).

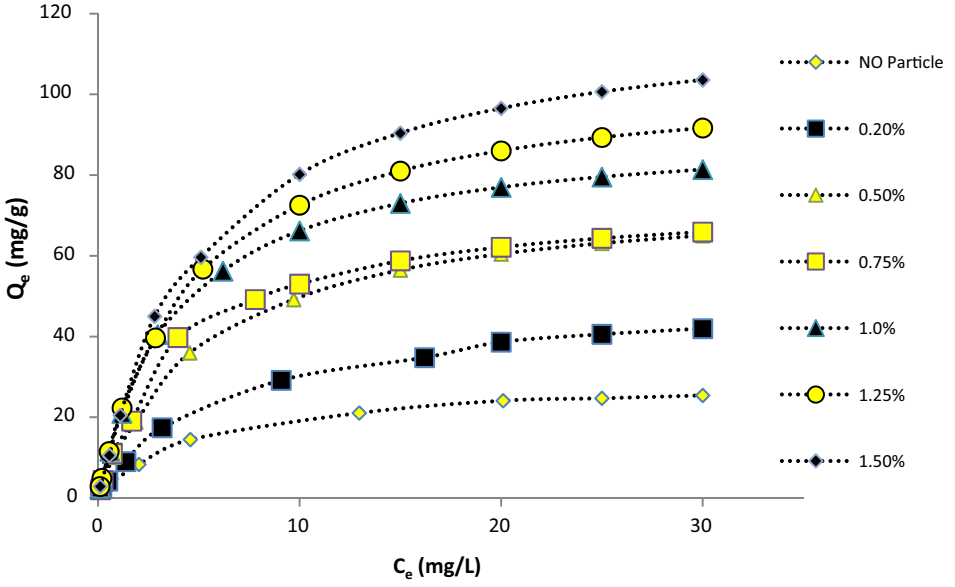

Fig. 6 Equilibrium adsorption of Pb(II) on CS/PVA membranes with different DNDs content.

area. The images showed that addition of 1 wt% DNDs increases the porosity of the CS/PVA membrane but 1.5 wt % DNDs causes a slight reduction in the porosity, as obvious from Fig. 4 h. According to the literature, it seems that low content of hydrophilic nanoparticles, accelerate evaporation rate, also increase the intensity of NaOH attack to the membrane (during detach from the glass), leading to formation of wrinkles and pores in the membrane structure during the preparation process (Salehi et al., 2013). On the other hand, higher amounts of nanoparticles results in compact membrane structures. Addition of 1.5% DNDs makes the membrane's structure to be denser than the plain membrane, which is due to high inter-connections of the polymeric matrix as well as increased viscosity of the casting solution (Salehi et al., 2012; Salehi et al., 2013).

3.3. *Effect of DNDs content*

The effect of DNDs content on the Pb(II) removal efficiency of CS/PVA/DNDs composite membranes (DNDs content varied from 0 to 1.5 wt%) was investigated. Fig. 5 exhibited the removal efficiency of Pb(II) ions versus residence time for CS/PVA membranes with different contents of nanodiamonds loading (for the initial heavy metal ions concentration of 30 ppm, at 30 °C and pH = 6). As can be observed, removal rate is high at early times of adsorption and by passing time, the

removal rate decreases. On the other hand, as the Fig. 5 shows the highest adsorption uptake occurs within the first three hours. During the first hours of the adsorption process, there are higher empty active sites throughout the membrane. Therefore, stronger ion adsorption would be caused through the surface chelating mechanism (Salehi et al., 2012). Then, the adsorption sites will be gradually occupied by the ions and so, the mass transfer driving force and the uptake rate decreases (Khan et al., 2017).

It is also clear that, by increasing DNDs content, the ion uptake increases on the membranes. Diamond nanoparticles increases the removal rate of Pb(II) due to the increase in the porosity of the membrane Fig. 4 and the affinity due to the presence of functional groups on the surface of DNDs. However, addition of extra DNDs (more than 1 wt%) has no meaningful effect. At higher amount of nanoparticles, they agglomerate on the surface of the membrane and thus, reduce the porosity. Accordingly, the membrane loses a number of active sites. This leads to no meaningful enhancement in adsorption capacity despite using higher amount of nanoparticles.

3.4. Effect of Pb(II) concentration on the equilibrium adsorption

The equilibrium adsorption of Pb(II) ions onto the prepared adsorptive membranes (CS/PVA-DNDs) at different initial ion concentrations was investigated. To examine the equilibrium adsorbed amount, the experiments were performed at 20 °C and pH = 6 with different initial concentrations of lead solution (1–30 mg/L). The pH of the solution was adjusted with standard HCl (0.1 M) and NaOH (0.1 M).

Fig. 6 shows that with increasing the initial concentration, the adsorption of metal ions increases. In fact, higher metal concentrations increases the driving force and improves the interactions between ions and active sites (Salehi et al., 2013). It can also be observed that the ion adsorption is increased by raising DNDs content in the membrane. It can be explained as follows: with the more content of DNDs, the higher functional groups would be available for lead ions to uptake. Increasing membrane porosity and excess surface area are other causes for the increased adsorption on the membranes with higher DNDs loading.

3.5. Adsorption isotherms

Equilibrium isotherms play crucial role in describing the equilibrium adsorption behavior of adsorbents. Two adsorption isotherms, Langmuir and Freundlich isotherm, were used to investigate Pb(II) adsorption equilibria. These two models are the most common isotherms used to describe the solid–liquid adsorption system (Luo et al., 2013). Langmuir equation can be represented as:

$$Q_e = Q_{max}\frac{bC_e}{1+bC_e} \quad (2)$$

where Q_e (mg/g) and C_e (mg/L) are equilibrium adsorption amount and metal concentration at equilibrium. Q_{max} (mg/g) is the maximum adsorption (namely, adsorption capacity) and b (L/mg) is the Langmuir isotherm constant. In this equation, it has been assumed that the surface of the adsorbent is homogenous with negligible interactions between adsorbing molecules (Ghaee et al., 2010).

Table 1 Equilibrium constants and correlation coefficients of Freundlich and Langmuir isotherms for adsorption of lead ions on nanocomposite CS/PVA adsorptive membranes.

	Langmuir Isotherm Constants		
Membrane (% DNDs)	b (L/mg)	Q_{max} (mg/L)	R^2
0%	0.2061	29.54	0.9979
0.20%	0.1604	50.70	0.9982
0.50%	0.1871	76.60	0.9989
0.75%	0.2408	75.05	0.9919
1.00%	0.2575	91.91	0.9996
1.25%	0.2197	105.60	0.9992
1.50%	0.1951	121.30	0.9975
	Freundlich Isotherm Constants		
	a (mg/g)	m	R^2
0%	6.18	0.468	0.9858
0.20%	8.34	0.547	0.9922
0.50%	12.85	0.606	0.9883
0.75%	14.73	0.602	0.9742
1.00%	18.35	0.633	0.9886
1.25%	18.79	0.680	0.9972
1.50%	19.27	0.717	0.9892

Freundlich isotherm supposes that adsorption happens in multi-layered heterogeneous surfaces. Moreover, based on its hypothesis, stronger bonding sites are occupied sooner (Luo et al., 2013). This model is expressed as:

$$Q_e = aC_e^m \quad (3)$$

where a and m are the Freundlich isotherm constants.

Both models are in good agreement with the equilibrium adsorption data; however, the Langmuir model shows a better fit based on the higher R^2 values. The calculated results for the Freundlich and Langmuir isotherms fitted to the equilibrium adsorption data are given in Table 1.

Isothermal study results Table 1 indicated that the raising of DNDs content from nil to 1.5 wt% resulted in enhancing the adsorption capacity of the adsorbent from 29.5 mg/g to 121.3 mg/g, respectively. It is worth mentioning that having desired mechanical resistance is another most important property for an adsorbent beside having high adsorption capacity. This criterion limits the application of the nanocomposite membranes with DNDs content higher than 1 wt%, as described before. Furthermore, the rate constant of the Langmuir isotherms (b) tabulated the highest value for the membrane with 1 wt% DNDs, indicating superior uptake rate on this optimal membrane adsorbent.

3.6. Thermodynamic and effect of temperature

Fig. 7 shows that the removal of Pb(II) ions from aqueous solution by the membrane is affected by the temperature i.e., the ion uptake increases slightly as the temperature increases. Membrane adsorption capacity increases from 56.2 mg/g at 20 °C to 63.05 mg/g at 40 °C. It is probably due to the endothermic nature of the adsorption process (Salehi et al., 2013). Enhanced rate of intraparticle diffusion of lead ion as well as changes in the size of the membrane pores are other presumable reasons for the temperature effect (Shawky, 2009).

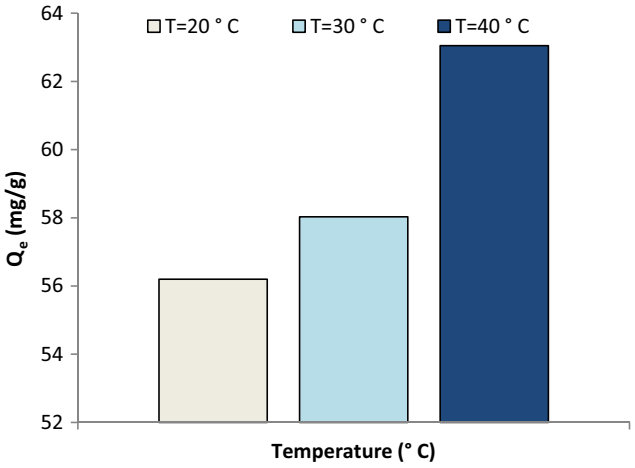

Fig. 7 Equilibrium isotherms for adsorption of lead ions on the membrane at various temperature (pH = 6).

Thermodynamic parameters including enthalpy change (ΔH^{o}), entropy change (ΔS^{o}) and Gibbs free energy change (ΔG^{o}) at different temperatures (20, 30 and 40° C) were obtained from Eqs. (4) and (5):

$$\ln K = \frac{\Delta S^{0}}{R} - \frac{\Delta H^{0}}{RT} \tag{4}$$

$$\Delta G = -RTlnK \tag{5}$$

where R is the universal gas constant, T (K) is the absolute temperature and k is the equilibrium adsorption constant which can be estimated by the rate constant of the Langmuir isotherm. The equilibrium adsorption constant demonstrates the relative distribution or partitioning of the solute between the aqueous phase and the adsorbent phase. K values can also be obtained from the intercept of the linear plot of $\ln(Q_e/C_e)$ against Q_e Fig. 8 (Salehi et al., 2012; Debnath et al., 2014).

The slope and intercept of the Van't Hoff's diagram, lnK versus $1/T$, represent enthalpy and entropy changes of adsorption, respectively. Gibbs free energy can be estimated from Eq. (5). Results of thermodynamic analysis are presented in Table 2.

Positive values of ΔH° show that the adsorption is endothermic. Positive values of ΔS° represent an increase in the randomness at the interface between the solid and liquid phases. It also shows well affinity between the cations and the membranes. Moreover, the randomness generated in the solid-liquid interface increases during the process of adsorption, which is probably due to the release of water molecules when hydrated lead ions is adsorbing on the surface of the adsorbent. Negative value of ΔG° indicates that the lead ion's adsorption is feasible and spontaneous. ΔG° decreases with increase in temperature, which is due to the endothermic nature of the process. This means the higher temperature, the more favorability of adsorption (Debnath et al., 2014).

3.7. Effect of pH

The solution pH has a great effect on the adsorption of components (Nesic et al., 2012). Fig. 9 shows the effect of pH on the adsorption of lead ions by CS/PVA/DNDs membrane. It can be seen that increasing pH from 4 to 6 enhanced the

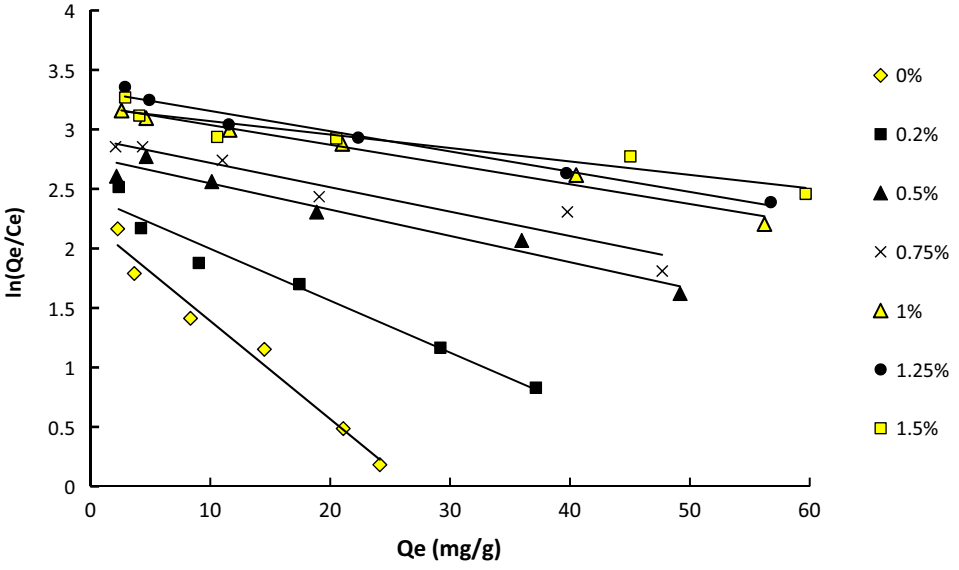

Fig. 8 ln(Qe/Ce) versus Qe for adsorption of Pb(II) on the membrane at various DNDs content.

Table 2 Standard thermodynamic parameters for adsorption of lead ions at different temperatures.

Membrane (M1)	ln K	ΔG° (kJ/mol)	ΔH° (kJ/mol)	ΔS° (kJ/mol)
T = 293 K	3.2025	−7.80	3.77	0.015
T = 303 K	3.3843	−8.525	...	...
T = 313 K	3.0994	−8.065	...	...

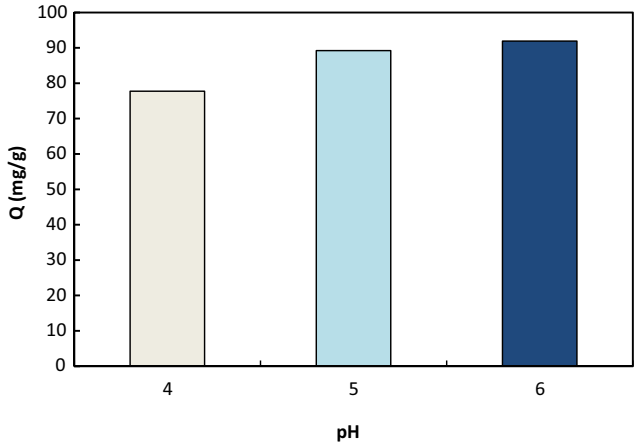

Fig. 9 Effect of pH on lead ions adsorption on the CS/PVA membrane containing 1 wt% DNDs.

adsorption capacity from 77 to 92 mg/g. In acidic pHs, competition between H_3O^+ and lead ions reduces the adsorption of the target ions (Salehi et al., 2013; He et al., 2008). The competition among the ions for amine adsorption sites through chelation mechanism is illustrated according to reactions (6)–(8):

$$R\text{-}NH_2 + H^+ \rightarrow R\text{-}NH_3^+ \quad (6)$$

$$R\text{-}NH_2 + Pb^{2+} \rightarrow R\text{-}NH_2Pb^{2+} \quad (7)$$

$$R\text{-}NH_3^+ + Pb^{2+} \rightarrow R\text{-}NH_2Pb^{2+} + H^+ \quad (8)$$

pH for pure adsorption (without precipitation) of most of metal ions on chitosan membranes is normally between 5 and 6 (Cheng et al., 2010; Liu and Bai, 2006; He et al., 2008; Boricha and Murthy, 2009). In acidic solution, the accumulation of protons on the membrane surface weakens the electrostatic interactions between the membrane surface and lead ions and therefore reduces the adsorption. Increased removal of lead ions in alkaline pHs is probably due to the formation of metal hydroxide (such as $Pb(OH)_2$) in the system. At such condition, sedimentation and precipitation promote the removal of metal hydroxide together with the adsorption mechanism (Cheng et al., 2010; He et al., 2008; Boricha and Murthy, 2009). Similar trends has been observed by other researchers for adsorption of metal ions on the chitosan membranes (Khan et al., 2017; Chen et al., 2009).

4. Conclusions

In this study, detonation diamond nanoparticles were employed, for the first time, to enhance the adsorption of the lead ion by CS/PVA thin membrane adsorbent. For this purpose, different contents of the nanoparticle were embedded in the matrix of the CS/PVA membranes. The optimum percentage of DNDs was 1 wt%; whereas, agglomeration of nanoparticles on the membranes surface was observed at 1.5 wt% of DNDs which caused a decrease in the porosity and mechanical stability of the membranes. It was concluded that extra addition of nanoparticle (> 1 wt%) could not significantly promote the membrane adsorption performance. It means that there is an optimum amount for the addition of DNDs into the CS/PVA matrix. Thermodynamic studies depicted spontaneous ($\Delta G^o < 0$), endothermic ($\Delta H^o > 0$) adsorption with entropy generation ($\Delta S^o > 0$) at the solid/liquid interface. The effect of solution pH on the adsorption capacity was also studied in the pH range of 4–6. The maximum adsorption capacity calculated by the Langmuir isotherm model was about 92 mg/g at 293 K and pH = 6. Generally, results suggested that the CS/PVA membranes including DNDs are excellent heavy metal adsorbers for application in water treatment process.

Acknowledgments

The authors thank the Kharazmi University and the Petrochemical Research and Technology Company for all of the support provided.

Conflict of interest

The authors declare that they have no conflict of interest.

References

Ridha, A.M., 2017. Removal of lead (II) from aqueous solution using chitosan impregnated granular activated carbon. J. Eng. 23 (3), 46–60.

Gupta, V.K., Agarwal, S., Saleh, T.A., 2011. Synthesis and characterization of alumina-coated carbon nanotubes and their application for lead removal. J. Hazard. Mater. 185 (1), 17–23.

Mehdipour, S., Vatanpour, V., Kariminia, H.-R., 2015. Influence of ion interaction on lead removal by a polyamide nanofiltration membrane. Desalination 362, 84–92.

Salehi, E., Madaeni, S., 2014. Influence of poly (ethylene glycol) as pore-generator on morphology and performance of chitosan/poly (vinyl alcohol) membrane adsorbents. Appl. Surf. Sci. 288, 537–541.

Salehi, E., Daraei, P., Shamsabadi, A.A., 2016. A review on chitosan-based adsorptive membranes. Carbohydr. Polym. 152, 419–432.

Jayakumar, R., Tamura, H., Prabaharan, M., Kumar, P.T.S., Nair, S. V., Furuike, T., 2011. Novel chitin and chitosan materials in wound dressing. In: Biomedical Engineering, Trends in Materials Science. InTech, pp. 1–22.

Shawky, H.A., 2009. Synthesis of ion-imprinting chitosan/PVA crosslinked membrane for selective removal of Ag (I). J. Appl. Polym. Sci. 114 (5), 2608–2615.

Cheng, Z., Liu, X., Han, M., Ma, W., 2010. Adsorption kinetic character of copper ions onto a modified chitosan transparent thin membrane from aqueous solution. J. Hazard. Mater. 182 (1), 408–415.

Liu, C., Bai, R., 2006. Adsorptive removal of copper ions with highly porous chitosan/cellulose acetate blend hollow fiber membranes. J. Membr. Sci. 284 (1), 313–322.

Jin, L., Bai, R., 2002. Mechanisms of lead adsorption on chitosan/PVA hydrogel beads. Langmuir 18 (25), 9765–9770.

Ashori, A., Bahrami, R., 2014. Modification of physico-mechanical properties of chitosan-tapioca starch blend films using nano graphene. Polym.-Plast. Technol. Eng. 53 (3), 312–318.

Delavar, Z., Shojaei, A., 2017. Enhanced mechanical properties of chitosan/nanodiamond composites by improving interphase using thermal oxidation of nanodiamond. Carbohydr. Polym. 167, 219–228.

Ghaee, A., Shariaty Niassar, M., Barzin, J., Matsuura, T., 2010. Effects of chitosan membrane morphology on copper ion adsorption. Chem. Eng. J. 165 (1), 46–55.

Khabashesku, V., Margrave, J., Barrera, E., 2005. Functionalized carbon nanotubes and nanodiamonds for engineering and biomedical applications. Diam. Relat. Mater. 14 (3), 859–866.

Khan, A., Begum, S., Ali, N., Khan, S., Hussain, S., Sotomayora, M. D.P.T., 2017. Preparation of crosslinked chitosan magnetic membrane for cations sorption from aqueous solution. Water Sci. Technol. 75, 2034–2046.

Vatanpour, V., Madaeni, S.S., Rajabi, L., Zinadini, S., Derakhshan, A.A., 2012. Boehmite nanoparticles as a new nanofiller for preparation of antifouling mixed matrix membranes. J. Membr. Sci. 401, 132–143.

Zarghami, S., Tofighy, M.A., Mohammadi, T., 2015. Adsorption of zinc and lead ions from aqueous solutions using chitosan/polyvinyl alcohol membrane incorporated via acid-functionalized carbon nanotubes. J. Dispersion Sci. Technol. 36 (12), 1793–1798.

Peng, S., Liu, Y., Xue, Z., Yin, W., Liang, X., Li, M., Chang, J., 2017. Modified nanoporous magnetic cellulose–chitosan microspheres for efficient removal of Pb (II) and methylene blue from aqueous solution. Cellulose 24 (11), 4793–4806.

Kyzas, G.Z., Siafaka, P.I., Lambropoulou, D., Lazaridis, N.K., Bikiaris, D.N., 2014. Poly (itaconic acid)-grafted chitosan adsorbents with different cross-linking for Pb (II) and Cd (II) uptake. Langmuir 30 (1), 120–131.

Weijiang, Z., Yace, Z., Yuvaraja, G., Jiao, X., 2017. Adsorption of Pb (II) ions from aqueous environment using eco-friendly chitosan schiff's base@ Fe3O4 (CSB@ Fe3O4) as an adsorbent; kinetics, isotherm and thermodynamic studies. Int. J. Biol. Macromol. 105, 422–430.

Lv, L., Chen, N., Feng, C., Gao, Y., Li, M., 2017. Xanthate-modified magnetic chitosan/poly (vinyl alcohol) adsorbent: preparation, characterization, and performance of Pb (II) removal from aqueous solution. J. Taiwan Inst. Chem. Eng. 78, 485–492.

Danilenko, V., 2004. On the history of the discovery of nanodiamond synthesis. Phys. Solid State 46 (4), 595–599.

Dolmatov, V.Y., 2001. Detonation synthesis ultradispersed diamonds: properties and applications. Russian Chem. Rev. 70 (7), 607–626.

Gerasin, V.A., Antipov, E.M., Karbushev, V.V., Kulichikhin, V.G., Karpacheva, G.P., Talroze, R.V., Raisa, V., Kudryavtsev, Y.V., 2013. New approaches to the development of hybrid nanocomposites: from structural materials to high-tech applications. Russian Chem. Rev. 82 (4), 303–333.

Mochalin, V.N., Shenderova, O., Ho, D., Gogotsi, Y., 2012. The properties and applications of nanodiamonds. Nat. Nanotechnol. 7 (1), 11–23.

Behler, K.D., Stravato, A., Mochalin, V., Korneva, G., Yushin, G., Gogotsi, Y., 2009. Nanodiamond-polymer composite fibers and coatings. ACS nano 3 (2), 363–369.

Zhang, X., Yin, J., Kang, Ch., Li, J., Zhu, Y., Li, W., Huang, Q., Zhu, Z., 2010. Biodistribution and toxicity of nanodiamonds in mice after intratracheal instillation. Toxicol. Lett. 198 (2), 237–243.

Krueger, A., 2008. The structure and reactivity of nanoscale diamond. J. Mater. Chem. 18 (13), 1485–1492.

Mitev, D., Dimitrova, R., Spassova, M., Minchev, Ch., Stavrev, S., 2007. Surface peculiarities of detonation nanodiamonds in dependence of fabrication and purification methods. Diam. Relat. Mater. 16 (4), 776–780.

Morimune, S., Kotera, M., Nishino, T., Goto, K., Hata, K., 2011. Poly (vinyl alcohol) nanocomposites with nanodiamond. Macromolecules 44 (11), 4415–4421.

Evarestov, R.A., 2012. LCAO calculations of perfect-crystal properties. In: Quantum Chemistry of Solids. Springer, pp. 357–488.

Lee, J.-Y., Lim, D.-S., 2004. Tribological behavior of PTFE film with nanodiamond. Surf. Coat. Technol. 188, 534–538.

Salehi, E., Mdaeni, S.S., Rajabi, L., Vatanpour, V., Derakhshan, A.A., Zinadini, S., Ghorabi, Sh., Ahmadi, H., 2012. Monfared, Novel chitosan/poly (vinyl) alcohol thin adsorptive membranes modified with amino functionalized multi-walled carbon nanotubes for Cu (II) removal from water: preparation, characterization, adsorption kinetics and thermodynamics. Sep. Purif. Technol. 89, 309–319.

Nesic, A.R., Velickovic, S.J., Antonovic, D.G., 2012. Characterization of chitosan/montmorillonite membranes as adsorbents for Bezactiv Orange V-3R dye. J. Hazard. Mater. 209, 256–263.

Salehi, E., Mdaeni, S.S., Rajabi, L., Derakhshan, A.A., Daraei, S., Vatanpour, V., 2013. Static and dynamic adsorption of copper ions on chitosan/polyvinyl alcohol thin adsorptive membranes: combined effect of polyethylene glycol and aminated multi-walled carbon nanotubes. Chem. Eng. J. 215, 791–801.

He, L., Wang, H., Xia, G., Sun, J., Song, R., 2014. Chitosan/graphene oxide nanocomposite films with enhanced interfacial interaction and their electrochemical applications. Appl. Surf. Sci. 314, 510–515.

Zuo, P.P., Feng, H.F., Xu, Z.Z., Zhang, L.F., Zhang, Y.L., Xia, W., Zhang, W.Q., 2013. Fabrication of biocompatible and mechanically reinforced graphene oxide-chitosan nanocomposite films. Chem. Cent. J. 7 (1), 39–50.

Han, D., Yan, L., Chen, W., Li, W., 2011. Preparation of chitosan/graphene oxide composite film with enhanced mechanical strength in the wet state. Carbohydr. Polym. 83 (2), 653–658.

Luo, C., Tian, Z., Yang, B., Zhang, L., Yan, Sh., 2013. Manganese dioxide/iron oxide/acid oxidized multi-walled carbon nanotube magnetic nanocomposite for enhanced hexavalent chromium removal. Chem. Eng. J. 234, 256–265.

Debnath, S., Maity, A., Pillay, K., 2014. Magnetic chitosan–GO nanocomposite: synthesis, characterization and batch adsorber design for Cr (VI) removal. J. Environ. Chem. Eng. 2 (2), 963–973.

He, Z., Nie, H., White, C.B., Zhu, L., Zhou, Y., 2008. Removal of Cu 2+ from aqueous solution by adsorption onto a novel activated nylon-based membrane. Bioresour. Technol. 99 (17), 7954–7958.

Boricha, A.G., Murthy, Z., 2009. Acrylonitrile butadiene styrene/chitosan blend membranes: preparation, characterization and performance for the separation of heavy metals. J. Membr. Sci. 339 (1), 239–249.

Chen, A., Yang, C., Chen, C., Chen, C.-Y., Chen, C.-W., 2009. The chemically crosslinked metal-complexed chitosans for comparative adsorptions of Cu (II), Zn (II), Ni (II) and Pb (II) ions in aqueous medium. J. Hazard. Mater. 163 (2), 1068–1075.